INT. J. NUM. METH. HEAT FLUID FLOW, VOL. 4, 189–206 (1994)

ALTERNATIVE DESIGNS TOWARDS THERMAL OPTIMIZATION OF COATED VALVES USING SPACE-TIME FINITE ELEMENTS*

UZI ZRAHIA AND PINHAS BAR-YOSEPH[$]

Computational Mechanics Laboratory, Faculty of Mechanical Engineering, Technion-Israel Institute of Technology, Haifa 32000, Israel

ABSTRACT

Heat transfer and stress analysis in metallic and coated exhaust valves are performed by an adaptive space-time finite element method. Results indicated that coatings of ordinary thickness cannot protect a coated valve operating in an uncooled engine. A new approach for designing the inner geometry of the metallic part in a coated hollow valve is presented. The purpose of the cavity is changed *from cooling to insulating*. Controlling the valve temperature and the heat flows out is done by changing the geometry of the cavity. The optimum is sought between the hollow geometry of the valve and its coating thickness while the outer geometry is that of an ordinary valve. Exhaust valves with optimal geometry are presented. A reduction of 40% of the heat flows out is obtained, compared to the heat flows out from a metallic valve operating in a cooled engine. By comparison, reduction of the heat flows out from a coated, ordinary geometry valve amounts to only 20%.

KEY WORDS Thermal optimization Exhaust valve Space-time elements

NOMENCLATURE

$\mathbf{A}$	finite element assembly operator
c	specific heat
$\mathbf{f}$	right hand side vector
G	solution domain
h	heat transfer coefficient; coating thickness
$\mathbf{K}$	coefficient matrix
L	axial thickness (defining the geometry of the valve cavity)
$\mathbf{n}$	unit normal vector
n_{dof}	number of degrees of freedom
n_{el}	number of elements
n_{en}	number of element nodes
N	basis function
P_1, P_2	optimization parameters
p	polynomial degree in the time and space directions
$\mathbf{q}$	heat flux vector
Q	heat loss
r	radial coordinate
t	time
T	exact solution for temperature
w	weighting function
z	axial coordinate

Greek letters

α	'switching' parameter in the analytic model
ΔT	temperature increment
Φ	angle (defining the geometry of the valve cavity)
Γ	boundary
η	refinement indicator
κ	thermal conductivity

* Dedicated to the Memory of Professor Arthur Stotter (1922–1992)

$ Corresponding author

0961–5539/94/030189–18$2.00

Received October 1992
Revised April 1993

ρ	density
Ω	space domain in the meridional cross section

Subscript

air	air cooled surfaces conditions
c	coating
f, u	water cooled surfaces conditions
gas	valve head facing combustion chamber conditions
s, j	exhaust gas conditions
m	metal, refinement level
Ref	reference value
∞	surrounding temperature

Superscripts

$\sim$	approximate value
e	element level
h	finite element approximation
n	nth time step
0	initial condition
$-$	average value

INTRODUCTION

Intensive research for the insulation of internal combustion engines was done during the early 1970s as part of the adiabatic engine concept. Insulation with ceramic coating enables a reduction of the metal parts temperature and increases the thermal efficiency of the engine. Ceramic coatings lead to temperature reduction in high engine loads, while in low engine loads it seems to have only a marginal effect on the temperature[1]. A fully insulated diesel engine was built by Cummins as part of the TACOM (Tank Automotive Command) project. The inner parts of the engine were coated with a 0.1 in layer of PSZ (Partially Stabilized Zirconia). This engine was operated without the cooling system[2].

One of the main disadvantages of the adiabatic engines concept is the limited coating thickness which can be obtained by present technology (1 mm approximately). In order to achieve good insulation a 5 mm coating thickness is required[3]. Analysis of the temperature field and the heat flows out from the inner parts of a diesel engine was carried out mainly in the following areas: (1) the iufluence of the ceramic coating on the temperature of metal parts and on the heat flows out through them; (2) the possibility of eliminating the cooling system by using ceramic coatings; (3) redesigning the metal parts together with ceramic coatings, in order to improve the mechanical performance of these parts.

The purpose of the present work is to redesign a coated exhaust valve in order to minimize the heat flows out from it. An exhaust valve was chosen as a study case because it operates under difficult conditions.

Thermal analysis, which includes heat flux and temperature field calculations at steady state from an uncooled valve, was performed using an electrical analogue[4]. The accuracy of the method was 2%. One of the earlier works dealing with numerical calculations of heat transfer through engine valves was carried out in Reference 5. A steady state thermal analysis of an uncoated regular valve was performed by a second order finite difference scheme. No optimal configurations were checked. Thermal analysis using a finite element method for the whole engine was carried out in Reference 6.

Numerical work was carried out by Bertodo and Sivakumaran[7] in order to evaluate the relation between the geometry of an uncoated valve and its stress field. An uncoated valve with an outer cavity in its centre was found to be a preferable configuration, and its maximum temperature was reduced by 50°C compared to a regular valve. The change in the heat transfer coefficient resulting from the change in geometry was not considered in that work.

A finite element analysis was carried out in order to define the steady heat flow and temperature fields in a valve with a zirconia layer applied to its head. This layer was covered by a thin layer of nickel alloy sheet metal. 50% of the heat flow from the combustion chamber side of the valve was blocked[8]. The main valves used today are summarized in Reference 9.

The above mentioned numerical works can be divided into two groups: the first deals with

optimization of the geometry of metal valves; the second deals with the correlation between ceramic coatings and the performance of valves.

In the present work, a combination of these two concepts is presented. This involves redesigning the metal geometry of a coated valve in order to minimize the heat flows out from it and thus to achieve an optimal valve. The optimum was carried out under maximum allowed temperature and stress constraints.

MATHEMATICAL FORMULATION

Weak formulation

The problem of heat transfer in an exhaust valve was solved for an axisymmetric configuration, under axisymmetric thermal loading (*Figure 1*) defined on a domain G such that:

$$G = \{(r, z, t):(r, z) \in \Omega \subset \mathscr{R}^2, t > {}^0t\} \tag{1}$$

where $\Omega \subset \mathscr{R}^2$ is an area domain with a piecewise smooth boundary $\Gamma = \Gamma_q \cup \Gamma_i$. Γ_q is a portion

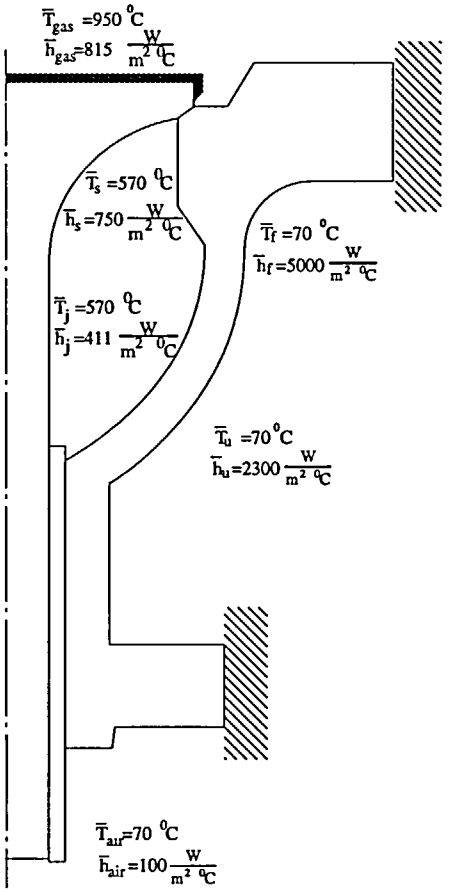

Figure 1 Solution domain with convection boundary conditions for a cooled engine

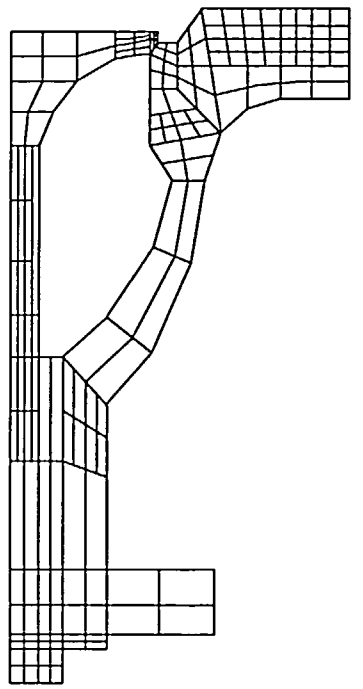

Figure 2 Adaptive finite element mesh for an uncoated exhaust valve

of the boundary over which convection boundary conditions are prescribed. Γ_i is a portion of the boundary which is thermally isolated. $\mathbf{x} = (r, z)$ is a set of cylindrical coordinates in Ω. It is assumed that the metal and coating materials are homogeneous and isotropic and that the heat transfer between the valve and surroundings occurs by convection only.

The energy equation in a cylindrical system of coordinates is given by:

$$\frac{1}{r}\frac{\partial}{\partial r}\left(r\kappa\frac{\partial T}{\partial r}\right)+\frac{\partial}{\partial z}\left(\kappa\frac{\partial T}{\partial z}\right)=\rho c\frac{\partial T}{\partial t} \quad \text{in } G \tag{2}$$

The initial and boundary conditions are:

Initial condition

$$T(\mathbf{x}, {}^0t) = {}^0T(\mathbf{x}) \quad \text{in } {}^0\Omega \tag{3}$$

Convection boundary condition

$$-\kappa\left(\frac{\partial T}{\partial r}n_r+\frac{\partial T}{\partial z}n_z\right)=\bar{h}(T-\bar{T}_\infty) \quad \text{on } \Sigma_q=\Gamma_q\times\,]{}^0t, t[\tag{4}$$

Isolation boundary condition

$$-\kappa\left(\frac{\partial T}{\partial r}n_r+\frac{\partial T}{\partial z}n_z\right)=0 \quad \text{on } \Sigma_i=\Gamma_i\times\,]{}^0t, t[\tag{5}$$

Applying the weighted residual method to (2)–(5) and Green's theorem both in space and time directions leads to the following weak formulation:

Given ${}^0T$, $\bar{T}_\infty$, and $\bar{h}$, find $\tilde{T}(\mathbf{x}, t)\in H_E^1(G)$ such that:

$$\int_G\left(\frac{\partial w}{\partial r}r\kappa\frac{\partial\tilde{T}}{\partial r}+\frac{\partial w}{\partial z}r\kappa\frac{\partial\tilde{T}}{\partial z}\right)\mathrm{d}G-\int_G\frac{\partial w}{\partial t}r\rho c\tilde{T}\,\mathrm{d}G$$
$$+\int_{\Sigma_q}wr\bar{h}(\tilde{T}-\bar{T}_\infty)\,\mathrm{d}\Gamma+\int_{{}^0\Omega}wr\rho cT\,\mathrm{d}\Omega-\int_\Omega wr\rho c\tilde{T}\,\mathrm{d}\Omega=0 \quad \forall w\in H_0^1(G) \tag{6}$$

where:

$$\begin{aligned}H_0^1(G)&=\{w\in H^1(G)\,|\,w(r,z,t)=0,\,(r,z)\in{}^0\Omega\}\\ H_E^1(G)&=\{\tilde{T}\in H^1(G)\,|\,\tilde{T}(r,z,t)={}^0T,\,(r,z)\in{}^0\Omega\}\end{aligned} \tag{7}$$

Space-time finite elements

Applying the finite element method in space and time[10,11], we first define at the nth time step a computational domain

$${}^nG:=\{(\mathbf{x},t):\mathbf{x}\in\Omega,\,{}^{n-1}t\leqslant t\leqslant{}^nt\} \quad n=1,2,\ldots$$

which is a subdomain of G, ${}^nt-{}^{n-1}t$ is the time length of ${}^nG$; the computational domain ${}^nG$ is broken up into n_{el} elements in the space direction and one element in the time direction. The elements are of order p in each direction. The lower and upper time boundaries of the eth element defined on ${}^nG^e$ are ${}^{n-1}\Omega^e$ and ${}^n\Omega^e$, respectively. The global approximation, $\tilde{T}$, defined on G is replaced in each element by an approximate variable T^h which is defined on ${}^nG^e$.

The space of approximation of the solution T^h is taken to be a subspace S^h of $H_E^1(G)$ consisting of all piecewise polynomials of degree $\leqslant p$ such that:

$$\mathrm{S}^h=\{\Phi\in H^1(G),\,\Phi|_{{}^nG^e}\in F_p({}^nG^e)\}\cap H_E^1(G)\}$$

where $F_p({}^nG^e)$ is the space of all polynomials of degree $\leqslant p$ on the element ${}^nG^e$.

A weighting function w^h is chosen, whose space is taken to be the subspace W^h of $H_0^1(G)$

consisting of all piecewise polynomials of degree $\leqslant p$ such that:

$$W^h = \{\Phi \in H^1(G), \Phi|_{{}^nG^e} \in F_p({}^nG^e)\} \cap H_0^1(G)\}$$

The finite element method applied to the weak formulation, (6), is as follows:

find an approximate solution $T^h \in S^h$ such that:

$$\sum_{e=1}^{n_{el}} \left\{ \int_{{}^nG^e} \left(\frac{\partial w^h}{\partial r} r\kappa \frac{\partial T^h}{\partial r} + \frac{\partial w^h}{\partial z} r\kappa \frac{\partial T^h}{\partial z} \right) dG - \int_{{}^nG^e} \frac{\partial w^h}{\partial t} r\rho c T^h \, dG \right.$$
$$\left. + \int_{\Sigma_q \cap {}^n\Sigma^e} w^h r\bar{h} T^h \, d\Sigma - \int_{{}^n\Omega^e} w^h r\rho c T^h \, d\Omega \right\}$$
$$= \sum_{e=1}^{n_{el}} \left\{ \int_{\Sigma_q \cap {}^n\Sigma^e} w^h r\bar{h} T_\infty) \, d\Sigma - \int_{{}^{n-1}\Omega^e} w^h r\rho c T^h \, d\Omega \right\} \quad \forall w^h \in W^h \tag{8}$$

Approximating the temperature at the eth element level by:

$$T^h(r, z, t) = \sum_{i=1}^{n_{en}} N_i^e(r, z, t) T_i^e \tag{9}$$

letting $w_i^h = N_i^e$, and substituting these expressions into (8) leads to the finite element formulation in the time and space directions. The basis functions N_i^e were chosen to be trilinear and triquadratic polynomials. The numerical evaluation of the integrations in (8) is performed by employing the Gauss–Lobatto quadrature. This formulation leads to a set of algebraic equations which for the nth time level can be written as:

$$\mathbf{K}\mathbf{T}^h = \mathbf{f}^h \tag{10}$$

here the vector $\mathbf{T}^h$ includes all the nodal points temperature values which are located in the space-time domain ${}^nG$; the temperature values at the nodal points which belong to ${}^{n-1}\Omega$ are evaluated from the previous time step, $n-1$, or from initial conditions for the case $n = 1$; and

$$\mathbf{K} = \mathop{\mathbf{A}}_{e=1}^{n_{el}} \mathbf{K}^e$$
$$\mathbf{f}^h = \mathop{\mathbf{A}}_{e=1}^{n_{el}} \mathbf{f}^e \tag{11}$$

A is the finite element assembly operator and

$$\mathbf{K}_{ij}^e = \int_{{}^nG^e} \left(\frac{\partial N_i^e}{\partial r} r\kappa \frac{\partial N_j^e}{\partial r} + \frac{\partial N_i^e}{\partial z} r\kappa \frac{\partial N_j^e}{\partial z} \right) dG - \int_{{}^nG^e} \frac{\partial N_i^e}{\partial t} r\rho C N_j^e \, dG$$
$$+ \int_{\Sigma_q \cap {}^n\Sigma^e} N_i^e r h N_j^e \, d\Sigma - \int_{{}^n\Omega^e} N_i^e r\rho C N_j^e \, d\Omega \tag{12}$$
$$\mathbf{f}_i^e = \int_{\Sigma_q \cap {}^n\Sigma^e} N_i^e r h T_\infty \, d\Sigma - \int_{{}^{n-1}\Omega^e} N_i^e r\rho C T^h \, d\Omega \quad 1 \leqslant i, j \leqslant n_{en}$$

The solution of the set of linear algebraic equations (10) was performed using a frontal solver[12]. The efficiency of this algorithm depends in which order the elements are numbered. A program, using Pina's algorithm[13], was written in order to achieve an optimal renumbering of the elements. The computations are performed by the finite element code FEAST[14] which is based on an adaptive space-time finite element program.

The initial conditions were taken as a uniform spatial distribution of the temperature,

${}^{0}T = 20°C$. The treatment of the average boundary conditions was carried out[4] for a medium-load 4-stroke diesel engine at 1500 rev/min and presented in *Figure 1*. For the uncooled engine, the boundary conditions within the cooling system were treated as free convection conditions. Within the cavity, insulation boundary conditions were assumed. A detailed analysis can be found in many works[4,15].

The approximate temperature field was used to calculate the thermal stress field within the valve. Using the virtual work principle[16], the displacement field was calculated at each time step. The stress field was obtained by using the Hook's law for isotropic homogeneous materials.

ADAPTIVE MESH

In order to save CPU time and computer storage an adaptive mesh was used. The adaptive mesh concept enables an automatic local refinement of the mesh in those domains in which the discretization error is high. The refinement procedure is based upon a refinement indicator which indicates on those elements to be refined.

Two adaptive mesh refinements have been tested: one is based on spatial redistribution of the nodal points at each time level (*r*-convergence). This can be done since according to formulation (8) the temperature can be approximated by discontinuous time finite elements. However, this approach needs a complicated procedure for projecting the approximate solution from the previous mesh onto the newly refined mesh. This process can yield highly distorted meshes. Alternatively, one can refine the mesh through subdividing all those elements in which the error indicator is greater than a given tolerance (*h*-type convergence). This approach yields meshes of elements having the same element aspect ratio and therefore, it has been finally adopted in the present study. A typical adaptive mesh for the valve is shown in *Figure 2*. Transition elements must be used since according to formulation (8), C^0 continuity is required for the spatial approximation of the temperature. Six transition elements have been used (*Figure 3*). The basis functions for these elements were chosen according to Reference 17.

A simple and effective error estimator should be considered for that problem. Zhu and Zeinkiewicz[18] showed for an elasticity problem an estimator based on the differences between a discontinuous calculated stress vector, $\hat{\sigma}$, and an interpolated continuous stress vector, σ^*. The

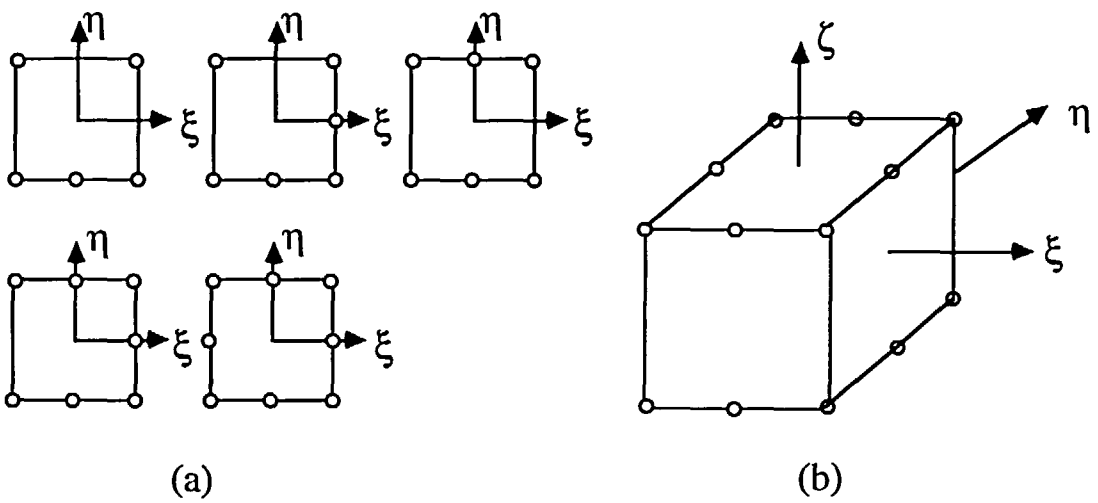

Figure 3 8–16 nodes transition elements: (a) upper view; (b) isometric view

approximating equation is achieved by a weighted residual requirement for equality between the two vectors[18]. The same procedure can also be employed in the present study for the heat flux. Other error estimators can be considered and more details on that subject can be found in References 19–21.

The refinement indicator in the present study was chosen as:

$$\eta^e = \int_{\Omega^e} \{(\nabla T^h)^T \kappa \nabla T^h\} \, d\Omega \tag{12}$$

where κ is the conductivity matrix. The integral in (12) is calculated exactly by using the Gauss quadrature.

The relation of the discretization error to the smoothness of the solution enables the use of a refinement indicator which is related to the heat flux and yields an automatic mesh refinement in the high heat flow regions. This is important in the present work where the optimization process of the valve is based upon the heat flux.

The adaptive procedure, for each time level, can be described as[19]:

1. Define an initial mesh ${}_mM$ and compute the finite element solution ${}_mT^h$ for this mesh ($m = 0$).
2. Using ${}_mT^h$ from the previous step compute the refinement indicator ${}_m\eta^e$, $e = 1, 2, \ldots, n_{el}$ in Ω^h.
3. Calculate the mean ${}_m\bar{\eta}$, and standard deviation ${}_ms$.
4. Define refinement intervals on the distribution of element indicators by considering the intervals:

$$ {}_mI^1 = {}_m(\bar{\eta}, \bar{\eta} + \beta s), \; {}_mI^2 = {}_m(\bar{\eta} + \beta s, \bar{\eta} + 2\beta s), \ldots, {}_mI^J = {}_m(\bar{\eta} + (J-1)s, \infty), $$

   where β represents the fraction of a standard deviation in each refinement interval. In the present study only one refinement interval which includes all the elements with indicators above the mean has been used.
5. Project the solution ${}_mT^h$ on the newly refined mesh ${}_{m+1}M$.
6. Calculate the temperature field ${}_{m+1}T^h$ for the new mesh and assign $m \leftarrow m + 1$.
7. Return to the second step and repeat the sequence of calculations until the mth refinement indicator is uniformly distributed in the spatial domain and the difference in solutions on successive meshes is small compared with a specified tolerance.

Testing of the adaptive algorithm

A two-dimensional steady state heat conduction problem was examined. The boundary conditions and the forcing terms were chosen such that the exact solution of the problem is:

$$T(x, y) = e^{-x} \cdot e^{-10y} \quad (x, y) \in]0, 1[\times]0, 1[\tag{13}$$

This solution has low gradients in the x direction and steep gradients in the y-direction (*Figure 4*). It was chosen due to the fact that the physical problem is expected to produce a similar temperature distribution near the coating layer. The initial mesh is constructed from sixteen trilinear elements. The automatic refinement of the mesh according to the present algorithm is shown in *Figure 5*. The error norms $\|e\|_{0,G}$, $\|e\|_{1,G}$ of the approximate solution in each mesh are presented in *Table 1* where $\|e\|_{0,G}$, $\|e\|_{1,G}$ are defined as:

$$\begin{aligned} \|e\|^2_{0,G} &= \int_G (T - T^h)^2 \, dG \\ \|e\|^2_{1,G} &= \int_G \left\{ (T - T^h)^2 + \left(\frac{\partial T}{\partial x} - \frac{\partial T^h}{\partial x} \right)^2 + \left(\frac{\partial T}{\partial y} - \frac{\partial T^h}{\partial y} \right)^2 \right\} dG \end{aligned} \tag{14}$$

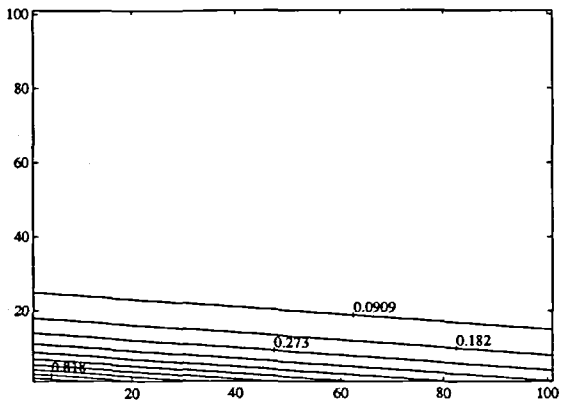

Figure 4 Exact temperature distribution for the test problem

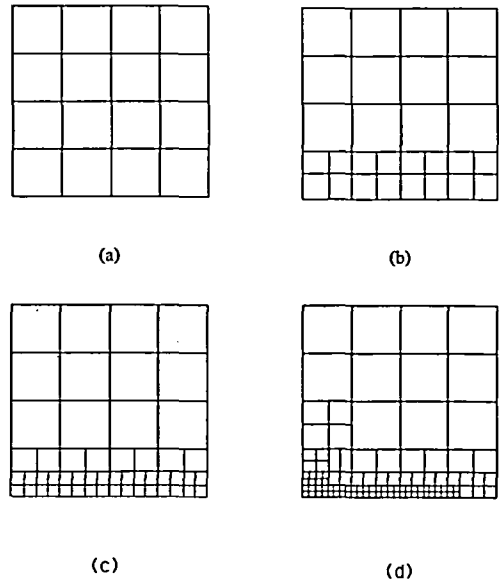

Figure 5 Finite element meshes for different refinement stages. (a) Initial mesh; (b) first refinement; (c) second refinement; (d) third refinement

Table 1 Normalized error norms *versus* number of degrees of freedom for the test problem

n_{dof}	Mesh no.	$\frac{\|e\|_{1,\Omega}}{\|T\|_{1,\Omega}}$	$\frac{\|e\|_{0,\Omega}}{\|T\|_{0,\Omega}}$
25	initial	0.172	0.166
42	first adaptation	0.099	0.054
75	second adaptation	0.054	0.036
146	third adaptation	0.041	0.028

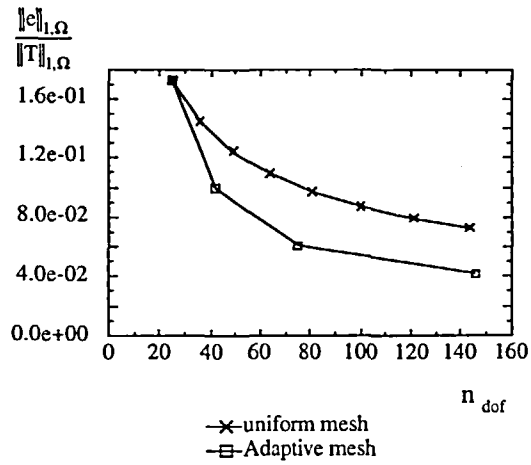

Figure 6 Normalized error norm *versus* the number of degrees of freedom for adaptive and uniform meshes

Comparison of the error obtained by using an adaptive mesh with that obtained by employing a uniform mesh is presented in *Figure 6*. For an equal number of degrees of freedom improved results are obtained with the adaptive mesh. Using the above adaptive procedure with the true error as a refinement indicator yields an error distribution which is very similar to the one depicted in *Figure 6*.

RESULTS

Temperature field in a valve: cooled engine

Coated and uncoated valves were considered in order to evaluate the correlation between the valve temperature and the coating thickness. An adaptive finite element mesh of an uncoated valve is presented in *Figure 2*. Average boundary conditions in the combustion chamber were used (*Figure 1*). A time dependent solution was calculated until the steady state temperature field was developed. The temperature field in an uncoated valve at different time levels, is shown in *Figure 7*. The location of the maximum temperature varied as a function of time. At steady state, the maximum temperature, $\text{Max}(T^h) = 598°C$, was found to be on top of the axis of symmetry, which is located far from the cooling system. This result is used in this work as a reference value.

In a coated valve, the temperature field was calculated using a range of coating thickness between 0.1 and 2.0 mm. The temperature field of a 0.5 mm coated valve is depicted in *Figure 8*. The maximum temperature of the metal was reduced by 70°C compared to an uncoated valve. Generally, the maximum ceramic temperature was observed to be on the edge of the valve, independent of time or coating thickness, since, at this point the right angle of the edge causes maximum thickness and the edge is exposed to heat flux from both r and z directions. This local high temperature creates a large thermal gradient which reduces the reliability of the ceramic coating and causes thermal singular stresses, which can result in failure of the coating. Reduction of the maximum temperature by 40°C was possible by recalculating the 0.5 mm coating configuration with a fillet corner.

Numerical calculations of the temperature field in valves of different coating thicknesses were performed in a similar way. A plot of the maximum temperatures *versus* coating thickness is presented in *Figure 9*.

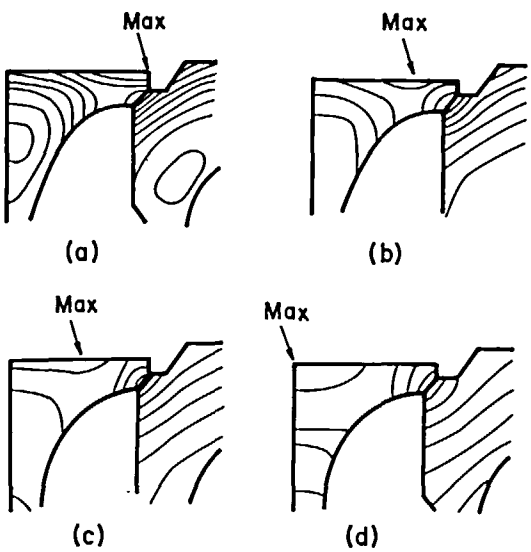

Figure 7 Isotherms for an uncoated valve at different time levels ($\Delta T = 19°C$). (a) $\max(T^h) = 140°C$, time = 15 sec; (b) $\max(T^h) = 237°C$, time = 25 sec; (c) $\max(T^h) = 334°C$, time = 35 sec; (d) $\max(T^h) = 598°C$, time = 165 sec

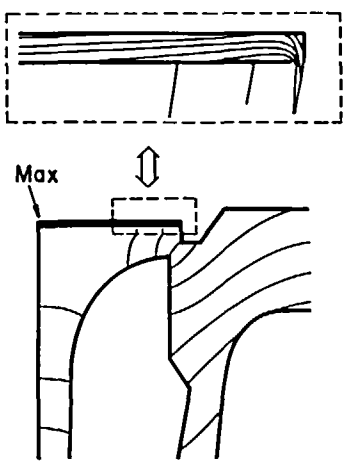

Figure 8 Isotherms for a valve with 0.5 mm coating thickness at steady state. Cooled engine: $\max(T^h) = 705°C$, $\Delta T = 19°C$

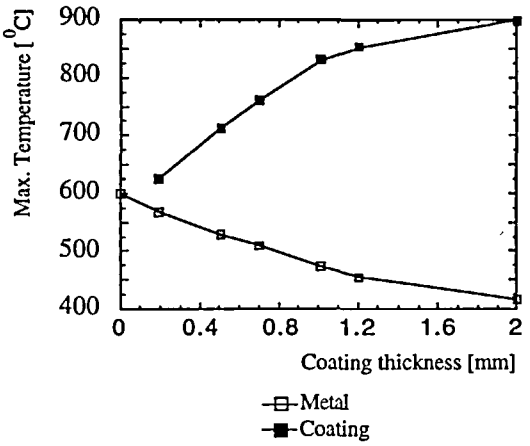

Figure 9 Maximal temperature in metal and ceramic at steady state *versus* coating thickness (cooled engine)

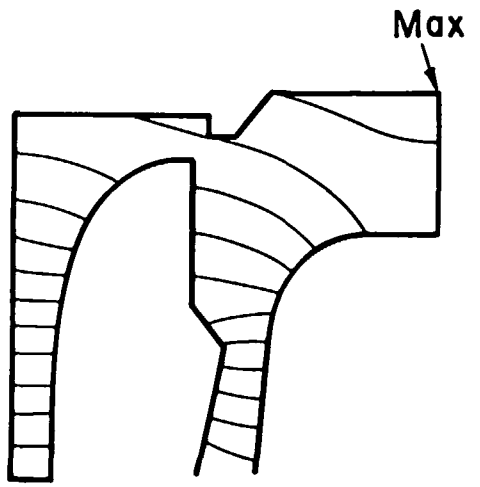

Figure 10 Isotherms at steady state. Uncooled engine: $\max(T^*) = 775°C$, $\Delta T = 18°C$

Temperature field in a valve: uncooled engine

Numerical solution. Elimination of the cooling system causes an increase in the metal temperature and should be compensated. The temperature field in an uncoated valve, working under uncooled engine conditions, was calculated in order to evaluate the valve temperature and its heat loss and to use these values for comparison purposes. The coating thickness required for the valve to operate in an uncooled engine was calculated. This was done under the constraint of the maximum allowable metal temperature.

The initial conditions are the same as those which had been used in the cooled engine. Boundary conditions of natural air convection were assumed in the cooling system. The maximum temperature at steady state in an uncooled and uncoated valve was found to be 757°C (*Figure 10*).

In order to find the influence of the coating thickness on the reduction of the metal temperature of the valve, the temperature in a coated valve with coating thicknesses of between 0.1 and 2.0 mm was calculated. The maximum metal temperature of a 0.7 mm coated valve was calculated to be 722°C. This value is still higher than the limit of 598°C. The correlation between the metal temperature and coating thickness in an uncooled engine is shown in *Figure 11*. The reduction rate of the metal temperature decreased as a function of coating thickness and after 1 mm its influence on the maximum temperature reduction was very small.

Analytic solution. From *Figure 10* it can be seen that the heat transfer in a valve, which operates in an uncooled engine, occurs mainly in the z direction. This fact was used to find an analytic model, simplifying the solution of the problem. The following two models are presented: one based on a one-dimensional model ($\alpha = 0$) and the second based on a fin model ($\alpha = 1$) (*Figure 12*).

In the coating, the temperature T_c satisfies:

$$\frac{d^2T_c}{dz^2} - \alpha\frac{\bar{h}_{gas}}{2r_1}(T_c - \bar{T}_{gas}) = 0 \quad \text{in } \Omega_c$$

$$-\kappa_c\frac{dT_c}{dz} = \bar{h}_{gas}(T_c - \bar{T}_{gas}) \quad \text{on } \Gamma_1 \tag{15}$$

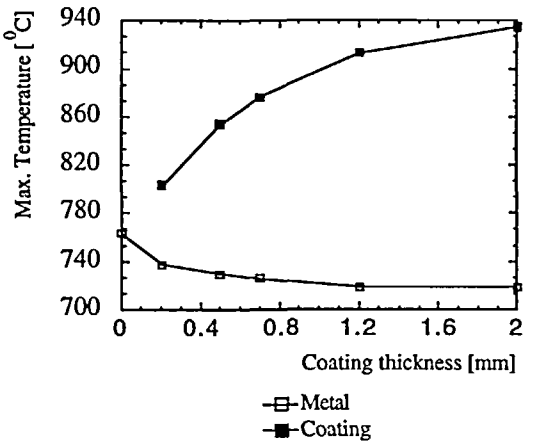

Figure 11 Maximal temperature in metal and ceramic at steady state *versus* coating thickness (uncooled engine)

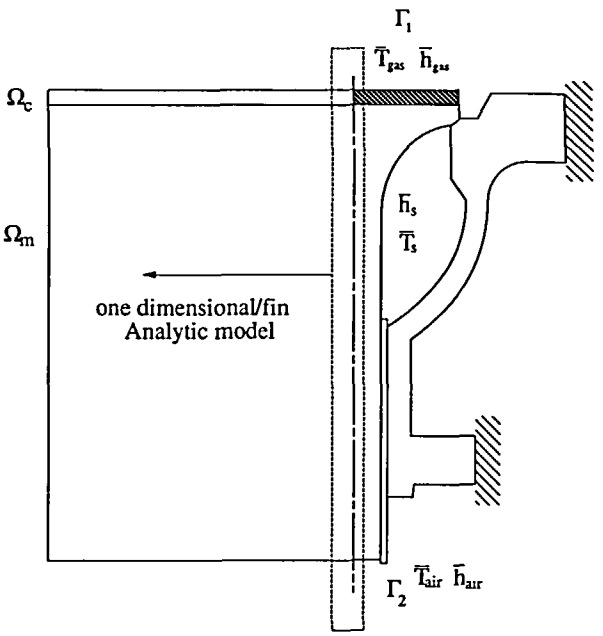

Figure 12 Analytic model for the valve based on a one-dimensional model

In the metal the temperature T_m satisfies:

$$\frac{d^2T_m}{dz^2} - \alpha\frac{\bar{h}_s}{2r_2}(T_m - \bar{T}_s)=0 \quad \text{in}\,\Omega_m$$
$$-\kappa_m\frac{dT_m}{dz} = \bar{h}_{air}(T_m - \bar{T}_{air}) \quad \text{on}\,\Gamma_2 \tag{16}$$

On the interface between the metal and coating, where $\Omega_m \cap \Omega_c$, the following conditions are imposed:

$$T_m = T_c$$
$$-\kappa_m\frac{dT_m}{dz} = -\kappa_c\frac{dT_c}{dz} \qquad \text{in}\,\overline{\Omega_m} \cap \Omega_c \tag{17}$$

The maximum metal and coating temperatures were calculated using the above formulation. The results of the one-dimensional model were higher than expected because this model neglects the heat loss from the fillet surface of the valve. Better results were obtained by the fin model which takes into account this heat loss (*Table 2*). These results show the good correlation between the analytic and the numerical models for the uncooled valve conditions. The analytic solution can be used in a preliminary design process only (e.g. as a first estimate of the maximum temperature within a coated valve).

OPTIMAL VALVE

It can be seen from the above temperature results for a regular valve that a ceramic coating cannot provide thermal protection of the metal parts in an uncooled engine under the limitation

Table 2 Temperature comparison based upon analytic and numerical solutions

Coating thickness (mm)	Numerical model temperatures (°C)		Analytic model temperatures (°C)			
			$\alpha = 1$		$\alpha = 0$	
	$T_{\Omega_c \cap \Omega_m}$	T_{Γ_1}	$T_{\Omega_c \cap \Omega_m}$	T_{Γ_1}	$T_{\Omega_c \cap \Omega_m}$	T_{Γ_1}
0.5	726	795	762	820	827	860
0.7	722	810	752	828	815	867
1.2	718	838	732	843	784	870
2.0	710	869	729	871	740	870

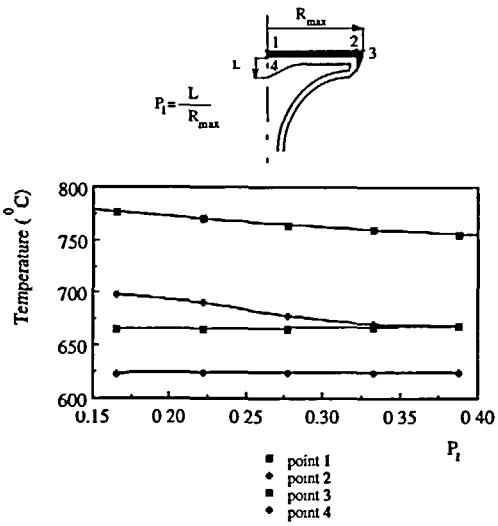

Figure 13 Parameter study for P_1–temperature at four sample points *versus* P_1

of a 2 mm coating thickness. This result leads to the conclusion that the research on ceramic coatings must be concentrated in the following two main directions:

(1) Use of ceramic coatings in cooled engines in order to reduce the metal temperature and thus enable the use of low quality metals.
(2) Redesigning the metal configuration of a coated valve in order to reduce the flows out heat flux. This heat loss reduction will be in addition to that which was achieved by coating a regular valve. The temperature of this valve will not be reduced as compared to an uncoated valve. The latter aim can be achieved by using hollow values which exist in special kinds of engines.

Usually the inner cavity is filled with sodium, which, by its motion, creates additional cooling[15]. The approach presented in this work is based on using hollow valves without sodium. Thus, the purpose of the cavity is changed *from cooling to insulating*. Controlling the valve temperature and the flows out heat flux is done by changing the geometry of the cavity.

An optimal valve must satisfy the following conditions: (1) minimum heat loss through it; (2) changing the valve geometry will not cause any change in other parts of the engine; (3) the valve temperature will not exceed the temperature of the reference valve. The reference valve is defined as an uncoated valve without cavities which operates in a cooled engine (*Figures 2* and *7*).

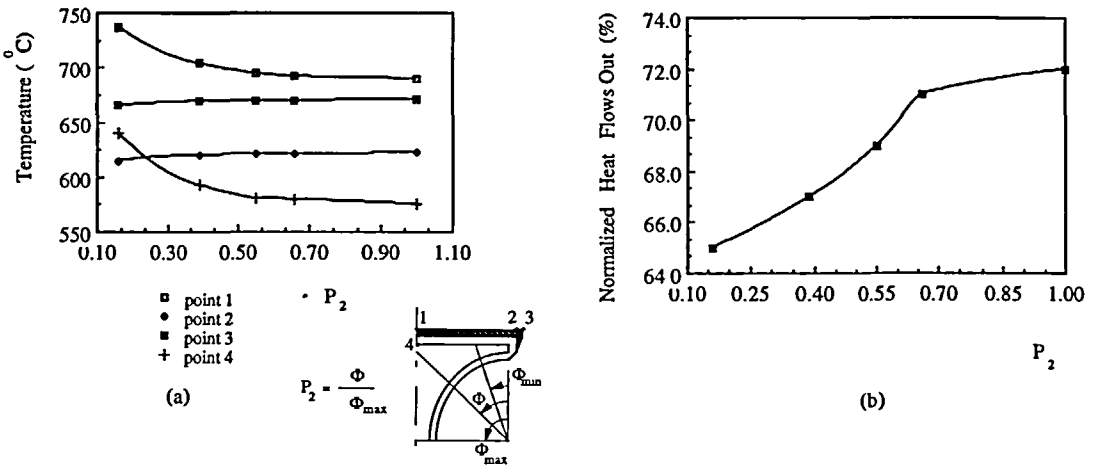

Figure 14 Parameter study for P_2. (a) Temperature at four sample points *versus* P_2; (b) normalized heat loss *versus* P_2

Two parameters, P_1 and P_2, have been defined:

$P_1 := L/R_{max}$—the rate between the metal thickness of the upper part of the valve (L) and its maximum radius, R_{max} (*Figure 13*).

$P_2 := \Phi/\Phi_{max}$—the rate between the angle Φ and the angle of maximum closed cavity, Φ_{max} (*Figure 14*).

The analytic solution is based on a one-dimensional model which cannot take into account the geometrical complexity of the hollow valve. Therefore the present optimization process is based on the proposed finite element procedure.

Variable P_1 *and* P_2 = *constant*, h = *0.5 mm*

Variation of P_1 was carried out in the range of 0.166–0.388. P_2 was set at its minimal value ($P_2 = 0.16$) in order to reduce its influence on P_1. The coating thickness, h, was set at 0.5 mm because this is the regular coating thickness which can be developed during one-pass spraying. First, a normalized heat flow was defined equal to the heat flows out from the valve divided by the heat flows out from the reference valve, i.e. Q/Q_{Ref}. The normalized heat flow does not change with respect to P_1. This can be explained by the fact that the heat transfer is mainly in the z direction, and changing P_1 does not influence the length of the effective area for heat transfer. The maximum metal temperature (at point 4) *versus* P_1 varies between 670°C and 700°C (*Figure 13*). These values, which are about 100°C higher than the temperature of the reference value, do not allow use of this configuration under the limitations of the optimization, as previously defined.

Variable P_2, P_1 = *constant*, h = *0.5 mm*

P_2 was sampled in the range of $0.16 < P_2 < 1.0$; P_1 was set at a middle value of 0.222 since this value has a negligible influence on Q/Q_{Ref}. Principally, it can be expected that increasing P_2 will cause a reduction in the valve temperature and an increase in the heat loss from the valve. Finding P_2 such that the maximum metal temperature will not exceed the maximum reference valve temperature (600°C) will give the optimal value.

Maximum metal temperature (at point 4) *versus* P_2 is presented in *Figure 14a*. The maximum metal temperature was reduced to a value of 593°C when P_2 was set to the value of 0.388. The

normalized heat loss (Q/Q_{Ref}) was equal to 67%. For comparison, Q/Q_{REF} was equal to 80% in a regular coated valve without cavities (*Figure 14b*). The temperature field for an optimal valve is shown in *Figure 15*.

Variable P_2, P_1 = *constant*, h = *0.9 mm*

Under the limitation of coating thickness, it is impossible to reduce P_2 below the value of 0.388 or the resulting normalized heat loss under 67%. The next step is to increase the coating thickness in order to obtain an optimal valve with higher efficiency. Setting $h = 0.9$ mm and reducing P_2 in the same way as above, enables better results (*Figure 16*). The normalized heat loss was reduced to a value of 62% and the maximum metal temperature was found to be 603°C.

The main valves which were tested are presented in *Table 3*. Choosing one of these valves depends on the design consideration in the following way. Valve 2 is chosen in order to allow

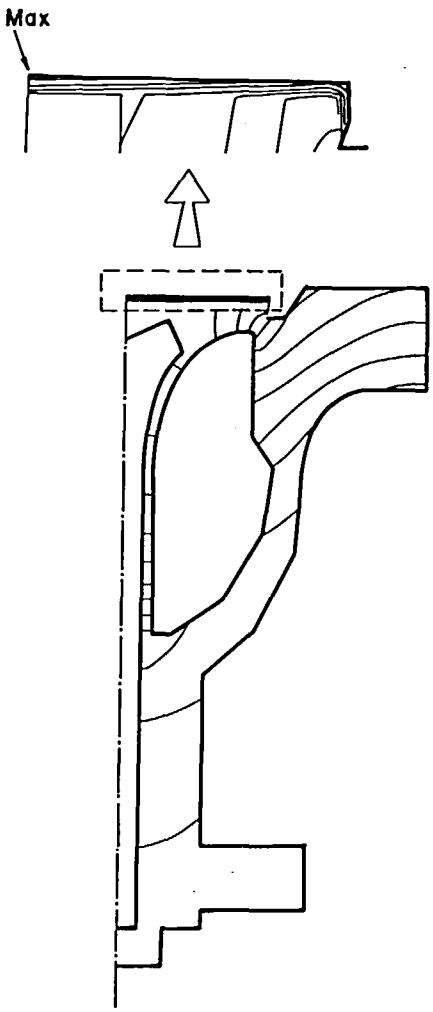

Figure 15 Temperature field in an optimal valve ($h = 0.5$ mm, $P_1 = 0.222$, $P_2 = 0.388$; $\max(T^h) = 704$°C, $\Delta T = 39$°C)

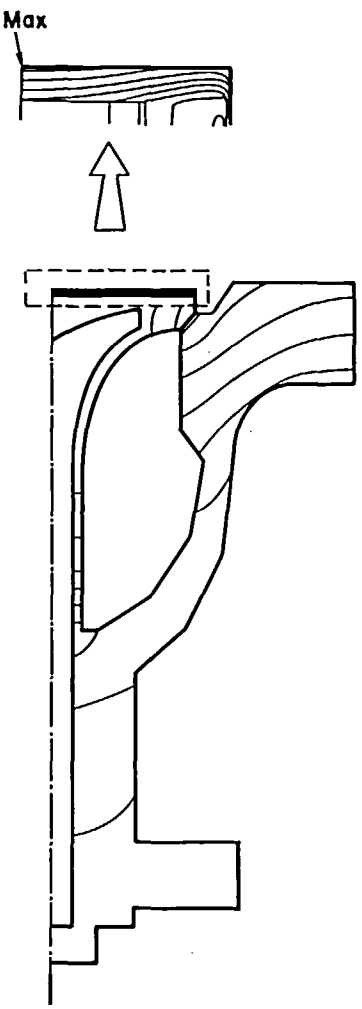

Figure 16 Temperature field in an optimal valve ($h = 0.9$ mm, $P_1 = 0.222$, $P_2 = 0.16$; $\max(T^h) = 759$°C, $\Delta T = 42$°C)

Table 3 Summary of main valves

No.	Valve type	Valve parameters P_1	P_2	h (mm)	Heat flows out from valve divided by heat flows out from reference valve Q/Q_{Ref} (%)	Maximal temperature in the metal part of the valve T_{max} (°C)
1	reference valve	—	—	0.0	100	598
2	regular coated valve	—	—	0.5	80	531
3		0.222	0.388	0.5	67	593
4		0.222	0.16	0.9	62	603

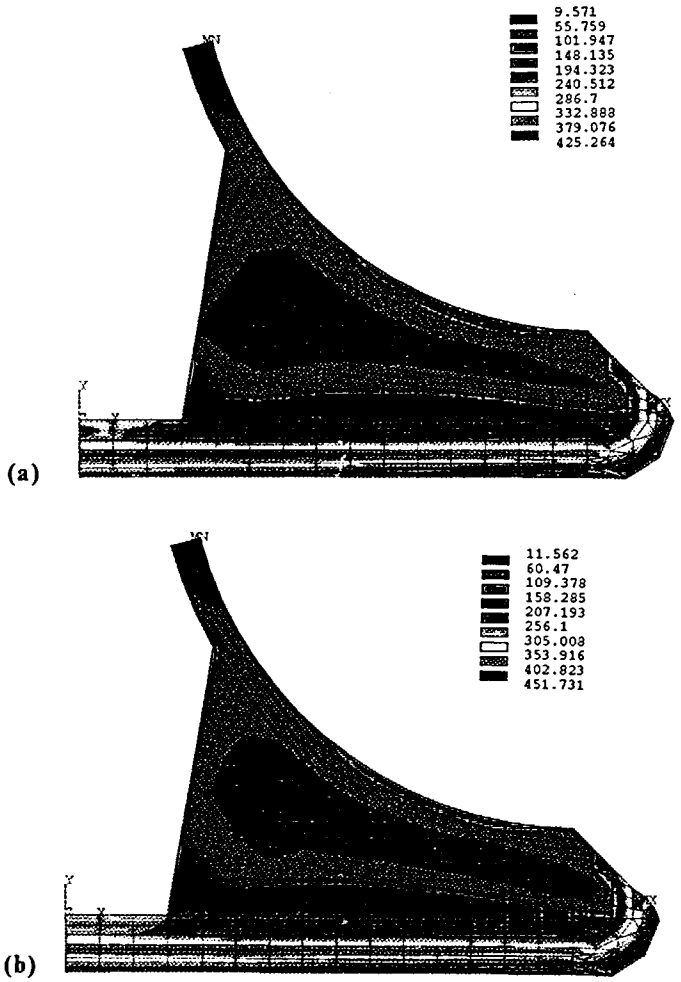

Figure 17 Stress field for two time levels (optimal valve; coating thickness = 0.9 mm). (a) Time = 40 sec; (b) steady state time, 160 sec

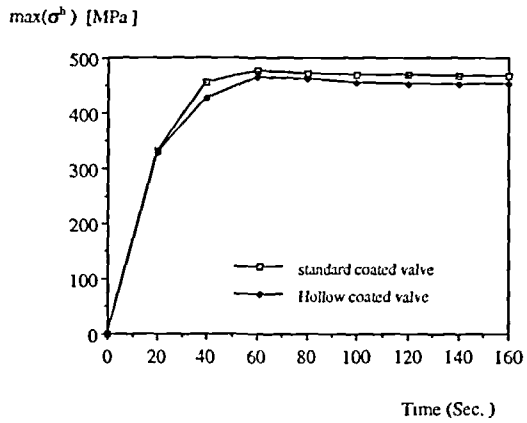

Figure 18 Comparison between the maximum equivalent stress in optimal and standard coated valves

the use of low quality metals. Valves 3 and 4 will be chosen in order to obtain high efficiency without reducing the metal temperature. The choice of any of these valves depends on mechanical considerations, i.e. the maximum allowed equivalent stress.

HEAT FLUX OPTIMIZATION STRATEGY

The mechanical-thermal design of an exhaust valve is summarized in the following flow chart (see Appendix). This algorithm was applied for a valve with the same properties as the previous valves. The stress fields for the optimized valve are shown in *Figures 17a* and *b* for two time levels. It is shown that the effect of the cavity on the magnitude of the maximum equivalent stress is negligible. A plot of the maximum equivalent stress *versus* the time is shown in *Figure 18*. The maximum stress profile is very similar both for regular and hollow valves. This is due to the fact that the high stresses are located at the interface between the metal and coating. Therefore, these stresses are mostly influenced by the mismatch in material properties and not from the geometry of the cavity.

CONCLUDING REMARKS

The following conclusions can be drawn:

(1) Coating thickness: coatings of ordinary thickness cannot protect an exhaust valve operating in an uncooled engine. Thus, an optimum must be sought between the inner geometry (cavity) of the metal and thickness of the coating.
(2) Cavity geometry: P_1 has a negligible influence on the normalized heat loss through the valve and on its temperature. Reducing P_2 enables one to decrease the heat loss from the valve while its maximum temperature is similar to this in the reference valve. Reduction by 40% of the heat flows out from an optimal valve is obtained, compared to the heat flows out from a metallic valve operating in a cooled engine, is obtained. By comparison, reduction by 20% of the heat flows out from an ordinary coated valve is obtained.
(3) Stress analysis was performed for all the valves which were considered during the optimization process. The cavity within the coated valve has a negligible effect on the magnitude of the maximum stress within it. The region of high stresses is located at the

interface between the coating layer and the steel. This value is mostly influenced by the mismatch in the material properties.

(4) The redesign of metallic parts combined with the use of ceramic coating allows higher efficiency of the coating's properties. This approach can be applied to other engine parts such as pistons.

(5) The numerical solution has the following features:
- The space–time convergence of the numerical solution has been examined for several test cases having analytic solutions. In all those cases the theoretical rate of convergence was confirmed.
- The mesh refinement procedure based on the proposed refinement indicator is found to be very efficient for generating adaptive meshes which are similar to the optimal one based on using the true error indicator.
- The present approach can be naturally extended for high order approximations by using the space–time spectral elements[22].
- The computatioual efficiency of the mesh refinement procedure can be increased by employing the switching function approach[23].

(6) Radiation from the sooting flame is an important fraction of the thermal load on an exhaust valve and thus should be considered[24]. The present model can be modified by replacing the convective boundary conditions with convection–radiation ones. However, it seems that the optimization trend will be similar to the one presented in this work.

(7) The high efficiency of the present approach makes it an important tool for designing internal combustion engines.

ACKNOWLEDGEMENTS

The cooperation of Dr S. Olek and the late Professor A. Stotter is gratefully acknowledged. This research was supported by Technion V.P.R. Fund—Col. Asher Peled Memorial Fund.

REFERENCES

1 Kvernes, I. Coating of diesel engine components, in *Coatings for High Temperature Applications* (Ed. E. Lang), Applied Science Publishers, London, pp. 384–392 (1986)
2 Bryzik, W. and Kamo, R. TACOM/Cummins adiabatic engine program, in *The Adiabatic Diesel Engine*, SP-543, Detroit, Michigan, pp. 21–46 (1983); (SAE-830314)
3 Kamo, R., Bryzik, W. and Grance, P. Adiabatic engine trends—worldwide, in *The Adiabatic Diesel Engine*, SP-700, Detroit, Michigan, pp. 1–14 (1987); (SAE-870018)
4 Stotter, A., Woolley, R. and Ip, E. S. Exhaust valve temperature—a theoretical and experimental investigation, *SAE-969A* (1965)
5 Janota, M. S., Hallam, A. J., Brock, E. K. and Dexter, S. G. The prediction of diesel engine performance and combustion chamber component temperatures using digital computers, *Proc. Inst. Mech. Eng.*, **182**, 58–69 (1968)
6 Wu, H. and Knapp, R. A. A heat transfer analysis of automotive internal combustion gasoline engines, in *Numerical Methods in Heat Transfer* (Eds. Lewis, R. W., Morgan, K. and Zienkiewicz, O. C.), Wiley, New York, pp. 511–527 (1981)
7 Bertado, R. and Sivakumaran, S. An assessment of diesel engine poppet valves, *Proc. Inst. Mech. Eng.*, **187**, 31–41 (1973)
8 Worlthen, R. P. and Tunnecliffe, T. N. Temperature controlled engine valves, *SAE-820501*, pp. 1091–2101 (1982)
9 Larson, J. M., Jenkins, L. F., Narsilmhan, S. L. and Belmore, J. E. Engine valves—design and material evaluation, *J. Eng. Gas Turbine Power* (*ASME Trans.*), **109**, 234–245 (1987)
10 Bonnerot, R. and Jamet, P. A second order finite element method for the one-dimensional Stefan problem, *Int. J. Num. Meth. Eng.*, **8**, 811–820 (1974)
11 Bonnerot, R. and Jamet, P. Numerical computation of the free boundary for the two-dimensional Stefan problem by space-time finite elements, *J. Comput. Phys.*, **25**, 163–181 (1977)
12 Taylor, C. and Hughes, T. G. *Finite Element Programming of the Navier–Stokes Equations*, Pineridge Press, Swansea, pp. 121–149 (1981)

13 Pina, H. L. G. An algorithm for frontwidth reduction, *Int. J. Num. Meth. Eng.*, 17, 1539–1546 (1981)
14 Zrahia, U. and Bar-Yoseph, P. *FEAST User's Manual*, Computational Mechanics Laboratory, Faculty of Mechanical Engineering, Technion, Haifa, Israel (1992)
15 Keriber, R. and Morel, T. Thermal shock calculations in I.C. engines, in *The Adiabatic Diesel Engine*, SP-700, Detroit, Michigan, pp. 223–241 (1987); (SAE 870162)
16 Zienkiewicz, O. C. and Taylor, R. L. *The Finite Element Method*, Vol. 1, 4th Edn, McGraw-Hill, New York, pp. 72–88 (1991)
17 McDill, J. M., Goldak, J. A., Oddy, A. S. and Bilby, M. J. Isoparametric quadrilaterals and hexahedrons for mesh-grading algorithms, *Commun. Appl. Num. Meth.*, 3, 155–166 (1987)
18 Zhu, J. Z. and Zienkiewicz, O. C. Adaptive techniques in the finite element method, *Commun. Appl. Num. Meth.*, 4, 197–204 (1988)
19 Carey, G. F. and Oden, J. T. *Finite Elements Computational Aspects*, Vol. III, Prentice-Hall, Englewood Cliffs, NJ (1984)
20 Rank, E. and Zienkiewicz, O. C. A simple error estimator in the finite element method, *Commun. Appl. Num. Meth.*, 3, 243–249 (1987)
21 Babuska, I., Zienkiewicz, O. C., Gago, J. and de Oliveira, E. R. (Eds.) *Accuracy Estimates and Adaptive Refinements in Finite Element Computations*, Wiley, New York (1986)
22 Zrahia, U. and Bar-Yoseph, P. Space–time spectral element method for solution of second order hyperbolic equations, *2nd Int. Conf. Spectr. High Order Meth., Montpellier* (1992); for publication in *Comp. Meth. Appl. Mech. Eng.*, accepted
23 Shpitalny, M., Bar-Yoseph, P. and Krimberg, Y. Finite elements mesh generation via switching function representation, *Finite Elements Anal. Des.*, 5, 119–130 (1989)
24 Morel, T. and Keribar, R. Heat radiation in diesel engines, *SAE 860445* (1986)

APPENDIX